

are the target molecules that undergo the additional poly(A) extension by TPAP in round spermatids.

It has been demonstrated that the deficiency of cytoplasmic polyadenylation element-binding protein (CPEB) results in the arrests of oogenesis and spermatogenesis at the pachytene stages (17). Although expression of two cytoplasmic polyadenylation element-containing mRNAs coding for the synaptonemal complex proteins SCP1 and SCP3 are unaffected by the CPEB deficiency, the poly(A) tails are reduced in length, and the protein products are missing in CPEB-deficient mice. In this study, the expression levels and sizes of CPEB, SCP1, and SCP3 mRNAs in *Tpap*<sup>-/-</sup> testes were similar to those in *Tpap*<sup>+/+</sup> and *Tpap*<sup>+/-</sup> testes (Fig. 3B). Moreover, no significant difference of the poly(A) tail size of SCP3 mRNA in pachytene spermatocytes was found between *Tpap*<sup>+/+</sup> and *Tpap*<sup>-/-</sup> mice. These data suggest that CPEB is not involved in the TPAP-mediated cytoplasmic polyadenylation. The null mutation of the TPAP gene does not affect the size or expression level of mRNAs encoding ovary-specific zona pellucida I (ZP1) and ZP2 (6) (fig. S3), verifying the testis-specific function of TPAP.

Western blot analysis of cytoplasmic and nuclear protein extracts from testicular tissues revealed that the level of TAF10 was reduced only in the nuclear fraction of *Tpap*<sup>-/-</sup> testes, whereas TBP, TAF12, TAF13, and TRF2 (16) were equally present in the cytoplasmic or nuclear fractions of *Tpap*<sup>+/+</sup> and *Tpap*<sup>-/-</sup> testes (Fig. 3C). The specific reduction of TAF10 was verified by immunoprecipitation analysis of the nuclear extracts with antibody to TBP (Fig. 3D). These data demonstrate that TPAP affects the transport of at least TAF10 into the nucleus, possibly by additional polyadenylation-dependent translational activation of dormant mRNA encoding a transporter protein or possibly by TPAP itself. Moreover, the poly(A) tails of TAF10, TAF12, and TAF13 mRNAs are unlikely to contribute to stability and translational control, because the levels of these three mRNAs and cytoplasmic proteins in *Tpap*<sup>-/-</sup> testes are comparable to those in *Tpap*<sup>+/+</sup> testes, despite the incomplete elongation of poly(A) tails (Fig. 3, A and C).

Several TAFs, including TAF10, as a component of the TFIID complex have been demonstrated to be dispensable for general RNA polymerase II-mediated transcription and to be essential for selective expression of specific genes (14, 18–22). Because the TFIID complex containing TAF10 is severely impaired in *Tpap*<sup>-/-</sup> testes by insufficient transport of TAF10 into the nucleus (Fig. 3, C and D), it is conceivable that TAF10 may play an important role in the expression of a subset of haploid-specific genes, possibly as a CREM coactivator (23), required for the morphogenetic program during spermatogenesis. However, a small

amount of TAF10, which probably forms the functional TFIID complex, seems to be still present in the nucleus of round spermatids in *Tpap*<sup>-/-</sup> mice (Fig. 3, C and D). Even if this is so, round spermatids appear to be incapable of producing enough mRNA to advance cell morphogenesis, because gene transcription (RNA synthesis) ceases around step-10 spermatids in the mouse (24). Our study shows a direct link between the deficiency of a cytoplasmic poly(A) polymerase, TPAP, and the arrest of mouse spermiogenesis, providing information on the regulation of haploid-specific genes by cytoplasmic polyadenylation in male germ cells.

References and Notes

1. A. B. Sachs, P. Sarnow, M. W. Hentze, *Cell* **89**, 831 (1997).
2. M. Wickens, P. Anderson, R. J. Jackson, *Curr. Opin. Genet. Dev.* **7**, 220 (1997).
3. N. B. Hecht, *BioEssays* **20**, 555 (1998).
4. K. Steger, *Anat. Embryol.* **199**, 471 (1999).
5. S. Kashiwabara et al., *Dev. Biol.* **228**, 106 (2000).
6. Materials and methods are available as supporting material on Science Online.
7. F. Nantel et al., *Nature* **380**, 159 (1996).
8. J. A. Blendy et al., *Nature* **380**, 162 (1996).
9. I. Martianov et al., *Mol. Cell* **7**, 509 (2001).
10. D. Zhang, T.-L. Penttila, P. L. Morris, M. Teichmann,

- R. G. Roeder, *Science* **292**, 1153 (2001); published online 12 April 2001 (10.1126/science.1059188).
11. W. Deng, H. Lin, *Dev. Cell* **2**, 819 (2002).
12. K. C. Kleene, *Development* **106**, 367 (1989).
13. S. Y. Han et al., *Biol. Reprod.* **64**, 507 (2001).
14. L. Tora, *Genes Dev.* **16**, 673 (2002).
15. S. Kashiwabara, Y. Arai, K. Kodaira, T. Baba, *Biochem. Biophys. Res. Commun.* **173**, 240 (1990).
16. S. Kashiwabara et al., data not shown.
17. J. Tay, J. D. Richter, *Dev. Cell* **1**, 201 (2001).
18. D. Metzger, E. Scheer, A. Soldatov, L. Tora, *EMBO J.* **18**, 4823 (1999).
19. S. R. Albright, R. Tjian, *Gene* **242**, 1 (2000).
20. Z. Chen, J. L. Manley, *Mol. Cell. Biol.* **20**, 5064 (2000).
21. R. N. Freiman et al., *Science* **293**, 2084 (2001).
22. M. A. Hiller, T.-Y. Lin, C. Wood, M. T. Fuller, *Genes Dev.* **15**, 1021 (2001).
23. G. M. Fimia, A. Morlon, B. Macho, D. De Cesare, P. Sassone-Corsi, *Mol. Cell. Endocrinol.* **179**, 17 (2001).
24. A. L. Kierszenbaum, L. L. Tres, *J. Cell Biol.* **65**, 258 (1975).
25. We thank L. Tora, I. Davidson, and T. Tamura for providing antibodies. This study was partly supported by Grant-in-Aids for Scientific Research on Priority Areas (A) and (B), Scientific Research (A), and Exploratory Research from the Japan Society for the Promotion of Science and the Ministry of Education, Culture, Sports, Science and Technology in Japan.

Supporting Online Material

www.sciencemag.org/cgi/content/full/298/5600/1999/DC1  
 Materials and Methods  
 Figs S1 to S4  
 References and Notes

3 June 2002; accepted 16 October 2002

## A Role for the Protease Falcipain 1 in Host Cell Invasion by the Human Malaria Parasite

Doron C. Greenbaum,<sup>1\*</sup> Amos Baruch,<sup>2</sup> Munira Grainger,<sup>4</sup> Zbynek Bozdech,<sup>2</sup> Katlin F. Medzihradzsky,<sup>1</sup> Juan Engel,<sup>3</sup> Joseph DeRisi,<sup>2</sup> Anthony A. Holder,<sup>4</sup> Matthew Bogyo<sup>2\*</sup>

Cysteine proteases of *Plasmodium falciparum* are required for survival of the malaria parasite, yet their specific cellular functions remain unclear. We used a chemical proteomic screen with a small-molecule probe to characterize the predominant cysteine proteases throughout the parasite life cycle. Only one protease, falcipain 1, was active during the invasive merozoite stage. Falcipain 1-specific inhibitors, identified by screening of chemical libraries, blocked parasite invasion of host erythrocytes, yet had no effect on normal parasite processes such as hemoglobin degradation. These results demonstrate a specific role for falcipain 1 in host cell invasion and establish a potential new target for antimalarial therapeutics.

Malaria is a devastating disease that affects 300 to 500 million people and kills about 2 million people per year. Currently, quino-

lines and antifolates are the most common drugs for disease prevention and cure. However, multidrug resistance is a major issue, highlighting the need for new antimalarial drugs to combat this parasite. Proteases represent one of the largest families of potential therapeutic targets, and cysteine proteases have been shown to be essential for the survival of several human parasites (1–3). Cysteine proteases have been specifically implicated in several cellular functions during the *P. falciparum* life cycle, including hemoglobin degradation (4–5), cleavage of red blood cell ankyrin to

<sup>1</sup>Department of Pharmaceutical Chemistry, <sup>2</sup>Department of Biochemistry and Biophysics, <sup>3</sup>Department of Pathology, Veterans Affairs Medical Center, University of California, San Francisco, CA 94143, USA. <sup>4</sup>Division of Parasitology, National Institute for Medical Research, Mill Hill, London NW7 1AA, UK.

\*To whom correspondence should be addressed at M. Bogyo, University of California, San Francisco, 513 Parnassus Avenue, San Francisco, CA 94043, USA. E-mail: dgreen@itsa.ucsf.edu (D.C.G.) and mbogyo@biochem.ucsf.edu (M.B.)

## REPORTS

facilitate host cell rupture (6), and the concomitant release of parasites from the parasitophorous vacuole (7). Furthermore, cysteine proteases are important for host cell invasion by *P. falciparum* and other related parasites (8, 9). However, the lack of a technically facile method to genetically manipulate the parasite has made functional analysis of key proteases difficult.

*P. falciparum* has a complex life cycle involving two distinct sexual and asexual stages of growth. The human asexual erythrocytic phase (blood stage) is the cause of most malaria-associated pathology and therefore is the focus of this study. The blood stage begins when merozoites (initially released from the liver) invade red blood cells. Over the next 48 hours, internalized parasites differentiate (ring stage), metabolize hemoglobin (trophozoite stage), and replicate (schizont stage) to produce expanded populations of invasive merozoites that are released upon rupture of the host cell (10). Merozoites have a limited life-span outside the host cell and must immediately find new cells to invade and start the cycle anew.

Initially, we used a functional proteomic method to identify and biochemically analyze all cysteine protease activity in extracts of *P. falciparum* (11–13). Four protease activities were detected in whole-cell lysates from mixed blood stages of *P. falciparum* parasites with the radiolabeled cysteine protease probe  $^{125}\text{I}$ -DCG-04 (Fig. 1A). One protease activity was enriched in an NP-40-insoluble pellet fraction, whereas the remaining protease activities remained soluble, suggesting distinct localization and/or biochemical properties of these enzymes.

The biotin affinity tag of DCG-04 afforded a single-step purification of all labeled proteins and their subsequent identification by mass spectrometry-based sequencing (Fig. 1B). Each of the proteases identified was a member of the papain family of cysteine proteases. Human calpain 1 was isolated from the NP-40-insoluble fraction but is not thought to play a functional role in *P. falciparum* (14). It is unlikely that this protease was purified as a result of contamination by red blood cells, because red blood cells were lysed before isolation of proteases with the probe. The purified cathepsin C-like protease matched a sequence found in the *P. falciparum* genome database (locus IDMal12P1.457) (15–17); however, no biological function for this enzyme has been reported. Falcipains 2 and 3 were also isolated from the NP-40-soluble extracts. These proteases reside in the food vacuole, where they play a critical role in hemoglobin degradation (4, 5). The remaining, detergent-insoluble

protease was identified as falcipain 1. Although falcipain 1 was the first cysteine protease gene cloned from the *P. falciparum* genome (18), difficulties in recombinant expression (19) have prevented its detailed biochemical and functional characterization. Thus, falcipain 1 is an ideal target for in situ studies with pharmacological tools to perturb its function.

To gain insight into the functional roles of specific cysteine proteases, we used highly synchronized parasite populations to profile protease activities throughout the multiple developmental stages of the parasite. For each stage, extracts were generated at pH 5.5, although analysis of falcipain 1, 2, and 3 activity indicated a broad pH activity profile. Cysteine protease activity was determined by labeling both detergent-

soluble and -insoluble lysates from each stage with  $^{125}\text{I}$ -DCG-04 (Fig. 1C). The activity profiles of falcipains 1, 2, and 3 indicated that regulation of these enzymes is highly divergent (Fig. 1D). Falcipain 2 and 3 activities peaked at the trophozoite stage, which is consistent with previously reported protein levels and with a role for these enzymes in hemoglobin degradation (4, 5). In contrast, falcipain 1 activity peaked during the merozoite stage and was the predominant protease activity in both the merozoite and the ring stages (Fig. 1D). This activity profile differs from the reported expression of falcipain 1 mRNA only in ring-stage parasites. This difference can be explained by both translational and post-translational mechanisms that control the maturation of falcipain 1 throughout the

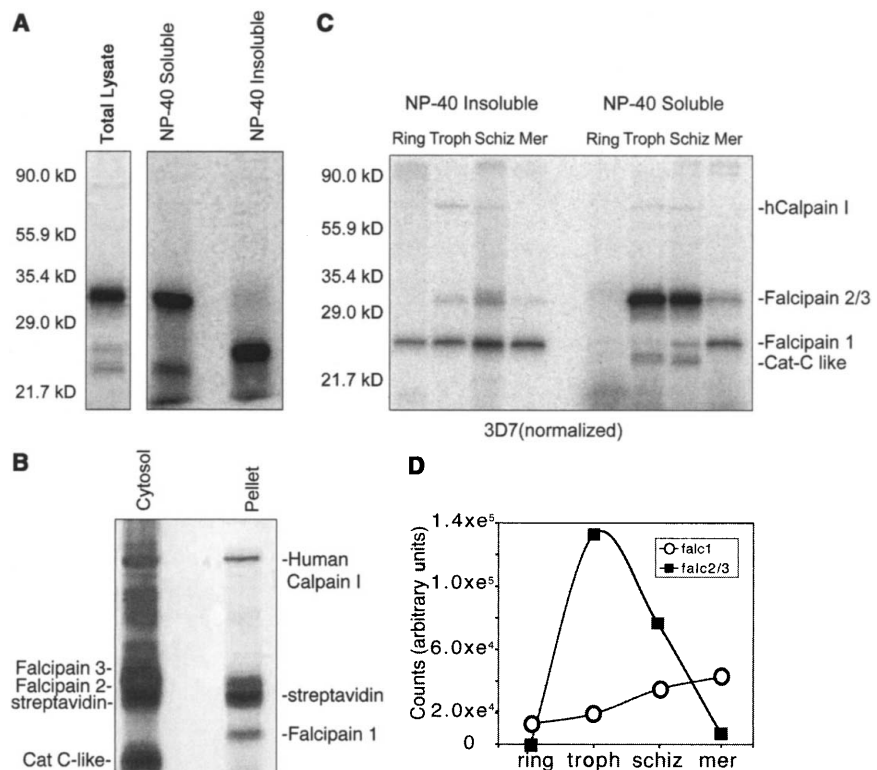


**Fig. 1.** Identification and biochemical characterization of active cysteine proteases within the erythrocytic cycle of *P. falciparum*. (A) Asynchronous cultures of *P. falciparum* parasites were isolated after sorbitol lysis of host red blood cells. Parasite pellets were lysed by addition of 0.2% NP-40, and total cellular extracts were labeled with  $^{125}\text{I}$ -DCG-04. Homogenates were separated on a 15% polyacrylamide gel, and labeled polypeptides were visualized with a PhosphorImager (total lysate lane). DCG-04-labeled parasite extracts were separated into 0.2% NP-40 soluble and insoluble fractions. Fractions were separated on 15% polyacrylamide gel and visualized by phosphorimaging. (B) Identification of affinity-labeled proteases. Parasite culture (1 liter) was harvested, lysed, and labeled with nonradioactive DCG-04. Probe-labeled proteases were affinity-purified by a single-step affinity purification protocol (9). Isolated proteases were excised by SDS-polyacrylamide gel electrophoresis (SDS-PAGE) and identified by in-gel trypsin digestion followed by mass spectrometry-based sequencing. Targets were identified by database (PlasmoDB) matching of peptide sequences. Cat C, cathepsin C. (C) Profiling protease activity throughout the erythrocytic life cycle. Synchronous parasites were harvested at the ring, trophozoite (troph), schizont (schiz), and merozoite (mer) stages. Lysates were separated into 0.2% NP-40 soluble and insoluble fractions and labeled with  $^{125}\text{I}$ -DCG-04. (D) Falcipain 1 and 2/3 protease bands from (C) were quantified with the ImageQuant software (Molecular Dynamics) and plotted for each of the major blood stages. Data for falcipain 1 represent a composite of insoluble and soluble activities.

## REPORTS

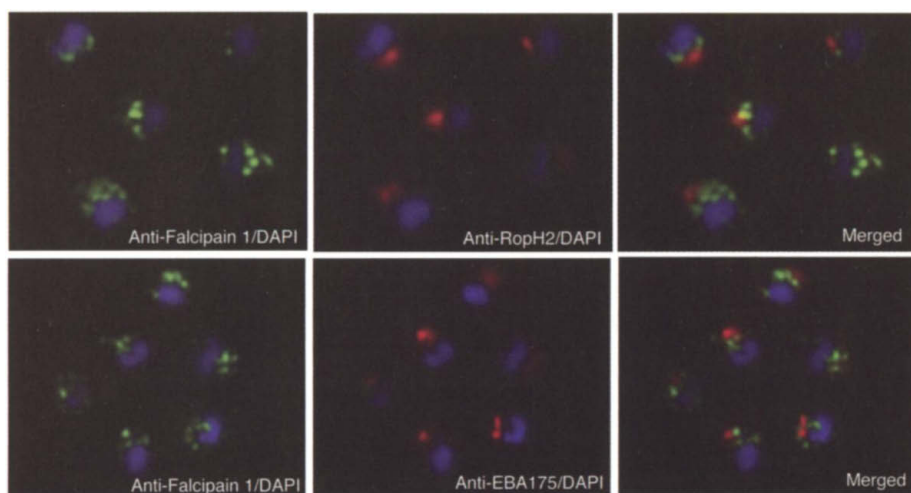


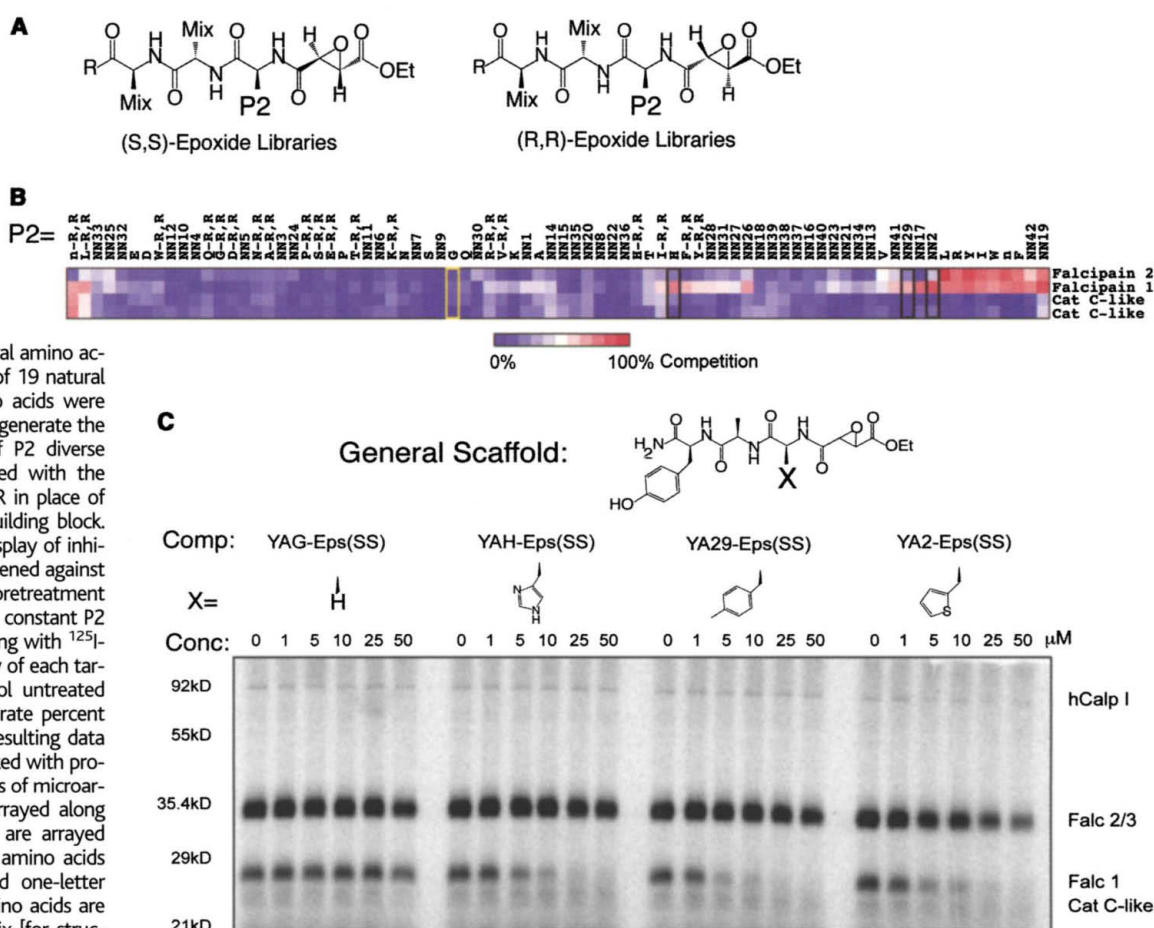
**Fig. 2.** Localization of falcipain 1 in merozoites by immunofluorescence imaging. Samples of merozoites were smeared and fixed in 1% paraformaldehyde. The slides were incubated with an antibody to falcipain 1 or with antibodies specific to the rhoptry (RopH2) and microneme (EBA-175) proteins. Nuclei were stained with 4',6-diamidino-2-phenylindole (DAPI). The lack of colocalization indicates that falcipain 1 is found in compartments at the apical end of the merozoite that are distinct from the rhoptries and micronemes.

life cycle of the parasite. This activity profile suggests a primary function for falcipain 1 either in red blood cell rupture or during reinfection of new host red blood cells.

In addition to having a distinct activity profile, falcipain 1 also changed its subcellular location during the late schizont and merozoite stages, as indicated by the appearance of an NP-40-soluble active form (Fig. 1C, far right lane). This soluble activity was most abundant in the merozoite stage and absent at the ring stage. During merozoite development, several new subcellular compartments are created that compose the apical organelles. These organelles participate in the process of host cell invasion through a controlled secretion of their contents (20). Localization of falcipain 1 to specialized compartments such as these may explain its change in detergent solubility. Furthermore, the short-lived, soluble falcipain 1 activity in merozoites could be explained by a mechanism in which active falcipain 1 is secreted during invasion.

To better understand the location and

**Fig. 3.** Identification of falcipain 1-specific inhibitors by screening peptide epoxide positional scanning libraries (PSLs) in crude cell extracts. (A) Structures of the general inhibitor scaffolds used for screening. A single amino acid position (P2) was held constant whereas the remaining positions contained an isokinetic mixture of natural amino acids (Mix positions). A set of 19 natural and 41 nonnatural amino acids were used at the P2 position to generate the libraries. A second set of P2 diverse sublibraries were generated with the enantiomeric form (2R, 3R in place of 2S, 3S) of the epoxide building block. (B) Colorimetric cluster display of inhibition data. PSLs were screened against *P. falciparum* lysates by pretreatment of samples with individual constant P2 libraries followed by labeling with <sup>125</sup>I-DCG-04. Labeling intensity of each target relative to the control untreated sample was used to generate percent competition values. The resulting data were clustered and visualized with programs designed for analysis of microarray data. Proteases are arrayed along the y axis and inhibitors are arrayed along the x axis. Natural amino acids are indicated by standard one-letter codes and nonnatural amino acids are labeled with the NN prefix [for structures and corresponding number assignment see (12, 13)]. Libraries generated with natural amino acids in the P2 position using the (R, R) scaffold are indicated by the single-letter code followed by (R, R). (C) Competition analysis of a negative control compound [YAG-Eps(S,S)] and three falcipain 1-specific compounds [YA2-Eps(S,S), YA29-Eps(S,S),



and YAH-Eps(S,S)] identified from library screening. Compounds were added to total parasite extract for 30 min followed by labeling with <sup>125</sup>I-DCG-04 for 1 hour. Samples were separated on a 15% SDS-PAGE gel. Comp, compound; Conc, concentration; Falc, falcipain; hCalp, human calpain.

## REPORTS

cellular function of falcipain 1, we used immunofluorescence-based localization studies with an antibody generated with a unique, COOH-terminal peptide sequence found in the mature enzyme. Immunoblots confirmed that these antibodies specifically recognized both the mature 26-kD enzyme and the larger proenzyme (21). The antibodies were then used in immunofluorescence assays of synchronized cultures to visualize the location of falcipain 1. Merozoites stained with an antibody to falcipain 1 revealed punctate staining in distinct vesicular structures at the apical end of the parasite, opposite the nucleus (Fig. 2, left panels). This punctate falcipain 1 staining pattern was also observed at the schizont stage, although it was excluded from the area of the food vacuole, further supporting a functional divergence from its close relatives falcipains 2 and 3 (22). In addition, co-staining was performed with antibodies to the rhoptry protein RopH2 and to the micronemal protein EBA-175, two of three invasion-specific organelles present only in merozoites (Fig. 2, middle panels). Merging of the two staining patterns indicated that the compartments containing falcipain

1 are distinct from the rhoptries and micronemes, yet localized to the apical end of the merozoite (Fig. 2, right panels). This unique staining of falcipain 1 implies localization to the third set of apical organelles, the dense granules, or to a subset of these organelles. The complement of subcellular compartments that compose the apical organelles may be more diverse than previously thought, and falcipain 1 might be located in a previously unidentified compartment. Ultimately, falcipain 1 localization to the apical end of the merozoite suggests a potential function in the invasion of red blood cells.

A more definitive analysis of falcipain 1 function requires application of methods that allow inhibition or disruption of its enzymatic activity in live parasite cultures. Gene ablation or knockout techniques have proven difficult in *P. falciparum*, and deletion of many genes from the haploid genome results in a lethal phenotype. An alternative chemical approach with a selective inhibitor that renders a specific target protease inactive allows dissection of the protease's biochemical function. Such a "chemical genetic" approach allows pheno-

typic evaluation at specific stages within the life cycle of the parasite.

To identify falcipain 1-specific inhibitors, we screened a positional scanning library of peptidyl epoxides (12, 13) in whole parasite lysates. We generated libraries by fixing a single amino acid residue on a tripeptide inhibitor scaffold while varying the remaining two positions (Fig. 3A). This method produces a series of sublibraries made up of several hundred compounds, each having a single different fixed amino acid residue (Fig. 3A). Inhibitor potency and selectivity were assessed by incubation of lysates with each inhibitor sublibrary, followed by reaction with the general cysteine protease activity-based probe  $^{125}\text{I}$ -DCG-04. The potency of specific inhibitor scaffolds was measured as a ratio of the percent residual labeled proteases after inhibitor treatment relative to an untreated control. For analysis, the inhibition data were displayed in a colorimetric format and clustered on the basis of similarities in inhibitor profiles using software for microarray analysis (23) (Fig. 3B). Several falcipain 1-specific P2 amino acid residues were identified (Fig. 3B, black rectangles) and were used to design a series of specific inhibitors. These optimized inhibitors and a control, inactive P2 glycine-containing inhibitor (Fig. 3B, yellow rectangle), were assayed in parasite extracts over a range of concentrations (Fig. 3C). The most selective of the resulting inhibitors, YA29-Eps(S,S), showed greater than 25-fold selectivity for falcipain 1 over all other cysteine proteases. Furthermore, at optimal concentrations of 5 to 10  $\mu\text{M}$ , we observed selective inhibition of falcipain 1. The compound YAG-Eps(S,S) showed no activity toward any of the protease targets and therefore served as a control for in situ inhibitor studies.

Effects of cysteine protease inhibition in live cultures of *P. falciparum* were determined by treating parasites with the general papain family protease inhibitor E-64d, with the falcipain 1-specific inhibitor YA29-Eps(S,S), or with the control inhibitor YAG-Eps(S,S) at 40 hours after invasion. After rupture (10 to 12 hours later), the percentage of surviving cells was calculated by counting parasites. As predicted, the control inhibitor YAG-Eps(S,S) had no effect on parasite growth, as measured by a constant number of schizonts and levels of ring-stage parasites comparable to those of dimethyl sulfoxide-treated cultures (Fig. 4A, gray bars, and 4B, left panel). Inhibition of all papain family proteases with E-64d resulted in a marked decrease in the number of new ring-stage parasites (Fig. 4A, maroon bars). This decrease was dose dependent and resulted from a block of

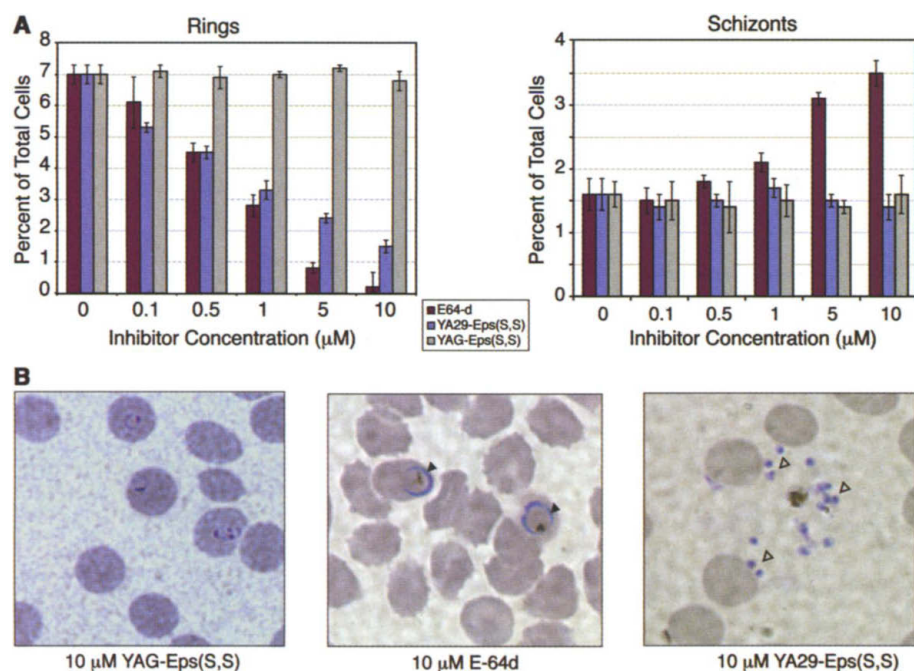


**Fig. 4.** Functional evaluation of falcipain 1-specific compounds in vivo. (A) Synchronous parasites (5% parasitemia) were treated with E-64d (maroon bars), with the falcipain 1-specific inhibitor YA29-Eps(S,S) (blue bars), or with the control inhibitor YAG-Eps(S,S) (gray bars) at the indicated concentrations 40 hours after invasion (late schizont stage). Smears were prepared at 58 hours after invasion. Ring- and schizont-infected red blood cells were counted as a percentage of total red blood cells. (B) Representative images of the parasites treated at the highest concentration (10  $\mu\text{M}$ ) of inhibitors from (A). The control compound YAG-Eps(S,S) had no effect on the parasites, as indicated by the presence of rings. The enlarged food vacuole of the schizonts in the E-64d-treated parasites (black arrowheads) is apparent. Falcipain 1-specific inhibitors such as YA29-Eps(S,S) blocked invasion but not host cell rupture, as seen by the lack of ring-stage parasites with normal release of merozoites (open arrowheads).

parasite development at the late schizont stage, as measured by an increase in schizonts. High concentrations of E-64d also induced a massive enlargement of the food vacuole within parasites, which is consistent with previously reported effects of general cysteine protease inhibitors (24) (Fig. 4B, middle panel). In contrast, falcipain 1-specific inhibitors caused a similar dose-dependent decrease in the percentage of new ring-stage parasites (Fig. 4A, blue bars), but did not block schizont development and subsequent rupture as indicated by the appearance of merozoites (Fig. 4B, right panel). Furthermore, schizont rupture was not affected, as assessed by the constant number of schizonts at all concentrations of falcipain 1-specific inhibitor (Fig. 4A) and by measurement of the release of the parasitophorous vacuolar protein SERA (serine repeat antigen) (25). These results suggest that falcipain 1 is not involved in hemoglobin degradation or red blood cell rupture at the end of schizogony, but rather has a specific role in the invasion of red blood cells by extracellular merozoites.

We have shown, using a functional proteomics screen combined with a chemical genetic approach, that falcipain 1 functions dur-

ing the process of host cell invasion during the erythrocytic cycle of *P. falciparum*. The primary sequence of falcipain 1 is well conserved across the *Plasmodium* genus (26), making it a potentially useful new target for design of therapeutic drugs in all four plasmodial species that cause malaria in humans. Therapeutic agents that are able to specifically prevent or slow the process by which merozoites infect new cells are likely to disrupt the development cycle and allow time for the host immune response to destroy the extracellular parasite.

References and Notes

1. P. J. Rosenthal, G. K. Lee, R. E. Smith, *J. Clin. Invest.* **91**, 1052 (1993).
2. J. H. McKerrow, J. C. Engel, C. R. Caffrey, *Bioorg. Med. Chem.* **7**, 639 (1999).
3. J. C. Engel, P. S. Doyle, I. Hsieh, J. H. McKerrow, *J. Exp. Med.* **188**, 725 (1998).
4. B. R. Shenai, P. S. Sijwali, A. Singh, P. J. Rosenthal, *J. Biol. Chem.* **275**, 29000 (2000).
5. P. S. Sijwali, B. R. Shenai, J. Gut, A. Singh, P. J. Rosenthal, *Biochem. J.* **360**, 481 (2001).
6. P. Raphael et al., *Mol. Biochem. Parasitol.* **110**, 259 (2000).
7. B. L. Salmon, A. Oksman, D. E. Goldberg, *Proc. Natl. Acad. Sci. U.S.A.* **98**, 271 (2001).
8. R. Mayer et al., *J. Med. Chem.* **34**, 3029 (1991).
9. X. Que et al., *J. Biol. Chem.* **277**, 25791 (2002).
10. L. H. Bannister, G. H. Mitchell, G. A. Butcher, E. D. Dennis, S. Cohen, *Cell Tissue Res.* **245**, 281 (1986).
11. D. Greenbaum, K. F. Medzhradzky, A. Burlingame, M. Bogyo, *Chem. Biol.* **7**, 569 (2000).

12. D. Greenbaum et al., *Mol. Cell Proteomics* **1**, 60 (2002).
13. D. Greenbaum et al., *Chem. Biol.*, **9**, 1085 (2002).
14. M. Hanspal, V. K. Goel, S. S. Oh, A. H. Chishty, *Mol. Biochem. Parasitol.* **122**, 227 (2002).
15. M. J. Gardner et al., *Science* **282**, 1126 (1998).
16. S. Bowman et al., *Nature* **400**, 532 (1999).
17. A. Bahl et al., *Nucleic Acids Res.* **30**, 87 (2002).
18. P. J. Rosenthal, R. G. Nelson, *Mol. Biochem. Parasitol.* **51**, 143 (1992).
19. F. Salas, J. Fichmann, G. K. Lee, M. D. Scott, P. J. Rosenthal, *Infect. Immun.* **63**, 2120 (1995).
20. C. E. Chitnis, M. J. Blackman, *Parasitol. Today* **16**, 411 (2000).
21. D. C. Greenbaum, M. Bogyo, unpublished data.
22. D. C. Greenbaum, J. Engel, A. A. Holder, M. Bogyo, unpublished data.
23. Cluster, version 2.11; TreeView, version 1.50, M. B. Eisen, P. T. Spellman, P. O. Brown, D. Botstein, *Proc. Natl. Acad. Sci. USA.* **95**, 14863 (1998) (available at <http://rana.lbl.gov>).
24. P. J. Rosenthal, J. H. McKerrow, M. Aikawa, H. Nagasawa, J. H. Leech, *J. Clin. Invest.* **82**, 1560 (1988).
25. D. Greenbaum, A. Holder, M. Bogyo, unpublished data.
26. P. J. Rosenthal, P. S. Sijwali, A. Singh, B. R. Shenai, *Curr. Pharm. Des.* **8**, 1659 (2002).
27. We thank J. McKerrow, P. Rosenthal, and C. C. Wang (University of California, San Francisco) for critical evaluation of the manuscript. Supported by funding from the Sandler Program in Basic Sciences (M.B.).

Supporting Online Material

[www.sciencemag.org/cgi/content/full/298/5600/2002/DC1](http://www.sciencemag.org/cgi/content/full/298/5600/2002/DC1)

Materials and Methods  
References and Notes

16 August 2002; accepted 15 October 2002

## Signaling of Rat Frizzled-2 Through Phosphodiesterase and Cyclic GMP

Adriana Ahumada,<sup>1</sup> Diane C. Slusarski,<sup>2</sup> Xunxian Liu,<sup>1</sup> Randall T. Moon,<sup>3</sup> Craig C. Malbon,<sup>1</sup> Hsien-yu Wang<sup>4\*</sup>

The Frizzled-2 receptor (Rfz2) from rat binds Wnt proteins and can signal by activating calcium release from intracellular stores. We show that wild-type Rfz2 and a chimeric receptor consisting of the extracellular and transmembrane portions of the  $\beta_2$ -adrenergic receptor with cytoplasmic domains of Rfz2 also signaled through modulation of cyclic guanosine 3',5'-monophosphate (cGMP). Activation of either receptor led to a decline in the intracellular concentration of cGMP, a process that was inhibited in cells treated with pertussis toxin, reduced by suppression of the expression of the heterotrimeric GTP-binding protein (G protein) transducin, and suppressed through inhibition of cGMP-specific phosphodiesterase (PDE) activity. Moreover, PDE inhibitors blocked Rfz2-induced calcium transients in zebrafish embryos. Thus, Frizzled-2 appears to couple to PDEs and calcium transients through G proteins.

The Wnt proteins are secreted signaling proteins that play diverse roles in cell polarity, cell proliferation, and specification of cell fate (1–3). Wnt proteins signal through *frizzled* (Fz) gene products (4, 5), members of the superfamily of G-protein-coupled receptors (GPCRs) (6–8). Wnt-Fz family members can be grouped into functionally distinct classes. Activation of the Wnt- $\beta$ -catenin pathway increases nuclear accumulation of the Lef-Tcf transcriptional coactivator  $\beta$ -catenin (1, 2, 9), thus activating transcrip-

tion (10–14). The Rfz2 receptor, by itself, transduces binding of Wnt-5A to increases in intracellular calcium release (15) and activation of calcium-calmodulin-dependent protein kinase II (16, 17) and protein kinase C (18) without appreciably activating the canonical Wnt- $\beta$ -catenin pathway. Because purified, active Wnt proteins are not available for analysis of Rfz2 receptor function, we engineered a chimeric receptor to substitute the three cytoplasmic loops and the COOH-terminal tail of the Rfz2 receptor for the

corresponding regions of the hamster  $\beta_2$ -adrenergic receptor ( $\beta_2$ AR) (19). The Rfz2 chimeric receptor, whose cytoplasmic domains display no similarity to that of  $\beta_2$ AR (fig. S1A) (20), is functional insofar as it couples to calcium mobilization (19) and to rapid activation of calcium-calmodulin-dependent kinase II (16), as does the wild-type Rfz2.

For functional analysis of Rfz2 signaling, we expressed the Rfz2 chimera in mouse totipotent F9 teratocarcinoma cells and in Chinese hamster ovary (CHO) cells that lack endogenous  $\beta_2$ AR. We identified stable transfectants expressing the Rfz2 chimera in CHO clones by reverse transcription (RT) and polymerase chain reaction (PCR) amplification (fig. S1B) (19, 20), immunoblotting with antibodies to  $\beta_2$ AR (fig. S1C) (19, 20), and specific binding of the  $\beta_2$ AR antagonist [<sup>125</sup>I]iodo-

<sup>1</sup>Department of Molecular Pharmacology, Diabetes and Metabolic Diseases Research Center, University Medical Center, SUNY–Stony Brook, Stony Brook, NY 11794–8651, USA. <sup>2</sup>Department of Biological Sciences, University of Iowa, Iowa City, IA 52242, USA. <sup>3</sup>Howard Hughes Medical Institute, Department of Pharmacology and Center for Developmental Biology, University of Washington School of Medicine, Seattle, WA 98195, USA. <sup>4</sup>Department of Physiology and Biophysics, Diabetes and Metabolic Diseases Research Center, University Medical Center, SUNY–Stony Brook, Stony Brook, NY 11794–8661, USA.

\*To whom correspondence should be addressed. E-mail: [wangh@pharm.sunysb.edu](mailto:wangh@pharm.sunysb.edu)